Finite difference schemes for second order systems describing black holes

Mohammad Motamed,[1,2] M. Babiuc,[2,3] B. Szilágyi,[2] H-O. Kreiss,[1,2] and J. Winicour[2,3]

[1]*NADA, Royal Institute of Technology, 10044 Stockholm, Sweden*

[2]*Albert Einstein Institute, Max Planck Gesellschaft, Am Mühlenberg 1, D-14476 Golm, Germany*

[3]*Department of Physics and Astronomy, University of Pittsburgh, Pittsburgh, Pennsylvania 15260, USA*

(Received 19 March 2006; published 6 June 2006)

In the harmonic description of general relativity, the principal part of Einstein's equations reduces to 10 curved space wave equations for the components of the space-time metric. We present theorems regarding the stability of several evolution-boundary algorithms for such equations when treated in second order differential form. The theorems apply to a model black hole space-time consisting of a spacelike inner boundary excising the singularity, a timelike outer boundary and a horizon in between. These algorithms are implemented as stable, convergent numerical codes and their performance is compared in a 2-dimensional excision problem.

DOI: 10.1103/PhysRevD.73.124008 PACS numbers: 04.25.Dm, 04.20.Ex, 04.30.Db, 95.30.Lz

I. INTRODUCTION

A primary goal of numerical relativity is the computation of gravitational radiation waveforms from binary black holes. Radiation produced in the inspiral and merger of binary black holes is expected to provide a strong signal for gravitational wave observatories. However, the simulation of black holes has proved to be a difficult computational problem. The importance of this challenging problem has recently spurred a fertile interaction between numerical relativity and computational mathematics. The classic computational treatment of hyperbolic systems has been directed at fluid dynamics and has been based upon first differential order systems. Certain formulations of Einstein's equations take a more natural second order form, notably the harmonic formulation [1,2] for which well-posedness of the Cauchy problem was first established [3]. Here we present theorems regarding the stability of several evolution-boundary algorithms for such second order systems which have direct application to the black hole problem.

Harmonic coordinates $x^\alpha = (t, x^i) = (t, x, y, z)$ have only recently been used in designing numerical codes [4–12]. They satisfy the curved space wave equation

$$\Box_g x^\mu := \frac{1}{\sqrt{-g}}\partial_\alpha(\sqrt{-g}g^{\alpha\beta}\partial_\beta x^\mu) = 0. \tag{1.1}$$

In harmonic coordinates, Einstein's equations reduce to 10 quasilinear wave equations for the components of the metric,

$$\Box_g g^{\mu\nu} = S^{\mu\nu}, \tag{1.2}$$

where $S^{\mu\nu}$ are nonlinear terms which do not enter the principal part. Thus the scalar wave equation

$$g^{\alpha\beta}\partial_\alpha\partial_\beta u = 0, \tag{1.3}$$

which has the same principal part, provides a fundamental testing ground for designing algorithms to treat the nonlinear gravitational problem (1.2). In a previous study [13], we used this scalar equation to develop evolution and boundary algorithms for a model one dimensional black hole excision problem. Here we extend these results to two dimensions. While the extension to 2D involves substantial new features, the generalization from 2D to 3D is quite straightforward. Thus our results are immediately applicable to algorithms for the harmonic gravitational Eqs. (1.2), as well as their generalization to include harmonic gauge forcing terms [14] and other related generalizations such as the $Z4$ formulation [15].

We treat (1.3) in the second order differential form, which has advantages for both computational efficiency and accuracy over first order formulations [16,17]. Although the system can be reduced to first order symmetric hyperbolic form [18], this has the disadvantage of introducing auxiliary variables with their associated constraints and boundary conditions. The second order form is also best suited to the analogous wave equations governing elasticity and acoustics. Elasticity theory is governed by a coupled system of wave equations which for simple cases is similar to (1.3), in which the spatial components g^{ij} are determined by the elastic moduli. In fact, some of the techniques utilized here have been developed in a recent computational study of the wave equations governing an elastic body [19]. The new ingredient introduced in the wave Eq. (1.3) arises from the nonvanishing mixed space-time derivatives arising from the components g^{it}. Such terms do not ordinarily appear in the wave equations governing elasticity theory because they are treated in the rest frame of the body but they would necessarily arise in treating acoustic waves propagating in a medium with nonuniform macroscopic motion. In general relativity, these mixed space-time components of the metric correspond to a nonvanishing "shift," which is an essential feature of the black hole problem. In the standard 3 + 1 description of space-time [20], the Cauchy hypersurfaces $t =$ constant are required to be spacelike so that they have a length element with Euclidean signature

$$d\ell^2 = h_{ij}dx^i dx^j. \tag{1.4}$$

The inverse spatial metric h^{ij}, satisfying $h^{ij}h_{jk} = \delta^i_k$, is related to the spatial components of the 4-metric determining the wave operator by

$$h^{ij} = g^{ij} - \frac{1}{g^{tt}}\beta^i\beta^j, \tag{1.5}$$

where β^i are the components of the shift. Here, the spacelike character of the Cauchy hypersurfaces requires that $g^{tt} < 0$.

The wave equation with shift has not received a great deal of attention outside of recent work in general relativity [6,10,13,21–23], although the important causal effect of the shift in the black hole excision problem has been recognized. This causal effect has been incorporated in a first order computational treatment of Einstein's equations by using upwind differencing for the shift terms, see e.g. [24]. Even before the computational problem is attempted, new mathematical features introduced by the shift must be dealt with in formulating a well-posed initial-boundary value problem. The operator $h^{ij}\partial_i\partial_j$ is by construction an elliptic operator defined by the spatial metric of the Cauchy hypersurfaces. However, the operator $g^{ij}\partial_i\partial_j$ is elliptic only when the shift is sufficiently small. The elliptic case arises when the operator ∂_t is timelike, i.e. when the evolution proceeds in a timelike (subluminal) space-time direction.

Without loss of generality, we set $g^{tt} = -1$ and write the 2D version of (1.3) as

$$(\partial_t^2 - 2(\beta^x\partial_x + \beta^y\partial_y)\partial_t - (a_1 - \beta^x\beta^x)\partial_x^2 - (c_1 - \beta^y\beta^y)\partial_y^2 - 2(b_1 - \beta^x\beta^y)\partial_x\partial_y)u = 0, \tag{1.6}$$

where $h^{xx} = a_1$, $h^{xy} = b_1$ and $h^{yy} = c_1$. The Euclidean property of h^{ij} requires

$$a_1 > 0, \qquad c_1 > 0, \qquad a_1c_1 - b_1^2 > 0. \tag{1.7}$$

The components of g^{ij} are $g^{xx} = a = a_1 - \beta^x\beta^x$, $g^{yy} = c = c_1 - \beta^y\beta^y$ and $g^{xy} = b = b_1 - \beta^x\beta^y$. In the subluminal case when $g^{ij}\partial_i\partial_j$ is an elliptic operator, the simplest second order accurate difference approximation to (1.6) is

$$W := (\partial_t^2 - 2(\beta^x D_{0x} + \beta^y D_{0y})\partial_t - aD_{+x}D_{-x} - cD_{+y}D_{-y} - 2bD_{0x}D_{0y})u = 0. \tag{1.8}$$

(Here D_{0i}, D_{+i} and D_{-i} are, respectively, the centered, forward and backward difference operators in the x^i-direction defined in Sec. III). This leads to stable evolution-boundary algorithms for Dirichlet, Neumann, Sommerfeld or other dissipative boundary conditions. Stability was established for the 1D case using a semi-discrete energy norm in [13], and this was generalized using the discrete energy method to the full 3D case in [10,12].

The W-algorithm (1.8) is unstable when the shift is sufficiently large so that $g^{ii} \leq 0$ (for any diagonal component). This occurs in one of the strategies for avoiding problems with the singularity which ultimately forms inside a black hole. In this strategy, the singularity is "excised" by surrounding it with a spacelike inner boundary. The evolution direction which is adopted to this spacelike boundary is superluminal, so that g^{ij} no longer has Euclidean signature. In Sec. III, we establish the stability of several different second order, evolution-boundary algorithms for this superluminal case. For the Cauchy problem, we establish stability for a general system of wave equations in s spatial dimensions so that the results may be immediately applied to other second order systems such as elasticity theory or acoustics. For the boundary, we specialize our treatment to scalar equations in 2D in order to simplify the notation, but the extension to general systems in sD is straightforward. In particular, our results apply directly to the 3D harmonic evolution of black holes.

The analysis of the initial-boundary problem for (1.6) in Sec. III makes evident that the above geometric properties of the wave equation have a mathematical analogue which results independently from a consideration of the well-posedness of the problem. The geometrical and analytical approaches are complementary and provide a good meeting ground for the ideas of numerical relativity and computational mathematics. While the main concern of numerical relativity is the black hole problem, the stability theorems for the finite difference algorithms developed for the model problems considered here provide a firm basis for attacking this problem with the harmonic Einstein system (1.2).

In Sec. IV, we compare the performance of the algorithms for the superluminal case in a problem without boundaries. In Sec. V, we simulate a simple 2D model of the excision problem in which the inner boundary $\mathcal{S}$ is spacelike and the outer boundary $\mathcal{T}$ is timelike. Between the boundaries the operator $g^{ij}\partial_i\partial_j$ goes from nonelliptic to elliptic along a curve $\mathcal{H}$ where $\det(g^{ij}) = 0$. The metric is chosen so that no characteristics can leave the inner region between $\mathcal{S}$ and $\mathcal{H}$, so that $\mathcal{H}$ mimics the role of a horizon. The global simulation of (1.6) in the region bounded by $\mathcal{T}$ and $\mathcal{S}$ is achieved with a blended evolution algorithm. A stable superluminal algorithm is used in an inner region between $\mathcal{S}$ and $\mathcal{H}$. In the exterior region, this superluminal algorithm is blended to the W-algorithm (1.8), so that the W-algorithm is used to treat the outer boundary $\mathcal{T}$. This model excision problem involves many of the mathematical difficulties in the full gravitational case. We begin in Sec. II with some simple examples which illustrate the problem, its potential pitfalls and how to avoid them.

II. SOME SUBTLETIES ASSOCIATED WITH THE WAVE EQUATION WITH SHIFT

In an inertial coordinate system $\hat{x}^\alpha = (\hat{t}, \hat{x}^i)$ (in units where the velocity of light $c = 1$), the wave equation which governs special relativistic physics,

$$(\partial_{\hat{t}}^2 - \delta^{ij}\partial_{\hat{i}}\partial_{\hat{j}})u = 0, \tag{2.1}$$

does not contain a shift. The invariance of the velocity of light results from the property that this wave equation retains the same form (2.1) under a Lorentz transformation,

$$t' = \frac{1}{\sqrt{1-\beta^2}}(\hat{t} - \delta_{ij}\beta^i\hat{x}^j) \qquad x'^i = \frac{1}{\sqrt{1-\beta^2}}(\hat{x}^i - \beta^i\hat{t})$$
$$\beta^2 = \delta_{kl}\beta^k\beta^l, \tag{2.2}$$

to another inertial coordinate system with relative motion. In this way special relativity resolves the dilemma with experiment that under a Galilean transformation,

$$t = \hat{t} \qquad x^i = (\hat{x}^i - \beta^i\hat{t}), \tag{2.3}$$

(2.1) gives rise to the shifted wave equation

$$(\partial_t^2 - 2\beta^i\partial_i - (\delta^{ij} - \beta^i\beta^j)\partial_i\partial_j)u = 0 \tag{2.4}$$

whose solutions propagate with coordinate speeds in the range $|1 \pm \beta|$ (where $\beta^2 = \delta_{ij}\beta^i\beta^j$). This raises the question: why does the wave equation with shift arise in general relativity?

In fact, although there are no preferred inertial coordinates in general relativity, in any sufficiently small spacetime region it is always possible to introduce Gaussian coordinates in which the wave Eq. (1.3) reduces to the shift-free form

$$(\partial_t^2 - h^{ij}\partial_i\partial_j)u = 0. \tag{2.5}$$

The problem here is that in Gaussian coordinates the worldlines $x^i = \text{const}$ are geodesics, i.e. the worldlines of freely falling observers, which can be focused by the attractive nature of gravity to produce coordinate singularities. This can occur on a short time scale in a strong gravitational field.

Another reason for introducing a shift is the simplicity of harmonic coordinates in reducing Einstein's equations into the hyperbolic form (1.2). Since the shift components g^{it} satisfy a coupled system of nonlinear wave equations, even if they were initialized with vanishing Cauchy data they would in general evolve to be nonzero. This cannot be avoided by introducing a harmonic gauge forcing term, of the form $\Box x^\alpha = F^\alpha$, without choosing the forcing term F^α to depend upon the derivatives of the metric $\partial_\mu g^{\alpha\beta}$. This in turn jeopardizes the hyperbolic form of the reduced Einstein equations and the well-posedness of the Cauchy problem [14].

Yet another reason for introducing a shift arises in the simulation of black holes. Once a black hole of mass M has formed there is at most a proper time of order M (in gravitational units) until a physical singularity is encountered. On the other hand, a simulation which provides gravitational waveforms of physical interest typically requires an evolution for a proper time of more than $100M$ in the exterior region. One strategy for accomplishing this is to excise the singularity by surrounding it with a spacelike inner boundary for the simulation domain, i.e. an inner boundary which moves at superluminal speed. If the evolution tracks the inner boundary then a superluminal shift must be used.

This can be illustrated by a spherically symmetric Schwarzschild black hole for which the wave Eq. (1.3) becomes

$$\left(\left(1 + \frac{2M}{r}\right)\partial_t^2 - \frac{4M}{r}\partial_t\partial_r - \left(1 - \frac{2M}{r}\right)\partial_r^2 - \frac{1}{r^2}\left(\partial_\theta^2 + \frac{1}{\sin^2\theta}\partial_\phi^2\right)\right)u = 0, \tag{2.6}$$

in ingoing Eddington-Finkelstein coordinates. Here the evolution takes place on the spacelike Cauchy hypersurfaces $t = \text{const}$ which are nonsingular for $r > 0$. The black hole is located at $r = 2M$, which is a characteristic hypersurface with the horizon property that no characteristics leave the region $r \le 2M$. The singularity is excised by evolving in a domain $R_1 \le r \le R_2$, where $0 < R_1 < 2M$ and $R_2 \gg 2M$. The shift has the radial component

$$\beta^r = \frac{1}{1 + \frac{r}{2M}} > 0. \tag{2.7}$$

The change in sign of the coefficient of ∂_r^2 in passing inside the horizon does not change the hyperbolicity of the wave equation but it changes its mathematical properties. Outside the horizon, the curves of constant (r, θ, ϕ) are timelike, as well as the outer boundary $r = R_2$. In the outer region $2M < r \le R_2$, the W-algorithm (1.8) provides a stable second order evolution-boundary algorithm for the wave equation [10,12,13].

Inside the horizon, the t-direction, as well as the inner boundary $r = R_1$ is spacelike, i.e. evolution on a grid with constant (r, θ, ϕ) proceeds outside the light cone. This effects the mathematical properties of the wave equation. As a result, in this domain, the W-algorithm is unstable. The alternative algorithms presented in Sec. III are stable inside the horizon. But the W-algorithm has better accuracy than these algorithms in the exterior region [10]. In the simulation of the model excision problem in Sec. V, a stable algorithm for the superluminal regime is blended to the W-algorithm in the exterior.

The Schwarzschild horizon has the property that characteristics can not exit from inside, but can enter from the outside. Near the horizon, the radial part of Schwarzschild wave Eq. (2.6) has the same qualitative features as the wave equation

$$(\partial_t - \partial_x)(\partial_t + x\partial_x)u = 0, \tag{2.8}$$

which has a horizon $x = 0$. One set of characteristics of (2.8) cross the horizon at $x = 0$ in the negative x-direction. The other set of characteristics are tangent to the horizon and *diverge* away on either side. An observer at $x > 0$ cannot see beyond the horizon at $x = 0$. This is the situ-

ation which we dealt with in a model 1D excision problem [13] whose treatment we generalize to 2D in Sec. V. However, it should be emphasized that the related equation

$$(\partial_t - \partial_x)(\partial_t - x\partial_x)u = 0 \tag{2.9}$$

has a different mathematical character. Although (2.9) is also hyperbolic and has a well-posed Cauchy problem, one set of characteristics *converge* toward the horizon at $x = 0$. These characteristics approach each other exponentially fast and, in general, the gradients become exponentially large near $x = 0$. This would lead to the focusing of a wave into formation of a shock. Although we do not treat this case in this paper, it is important to bear in mind that it would require different methods.

Boundaries introduce additional subtleties. First consider a timelike boundary, similar to the outer boundary $r = R_2 > 2M$ for the Schwarzschild wave Eq. (2.6). Since the evolution is timelike in the neighborhood of the boundary, the W-algorithm can be used. The stability of dissipative boundary conditions for the W-algorithm was established for 1D in [13] and extended to 3D in [12] by means of a semidiscrete energy method. However, such an energy estimate does not preclude exponential growth of a wave traveling between two boundaries. A simple example [7] arises from the repetitive blue shifting of a wave packet in special relativity reflecting back and forth between two plane boundaries, whose velocities $\pm v$ are controlled to be always toward the packet during reflection. After many reflections the wave packet shrinks in size and its energy grows by a factor $e^{4\alpha T}$, where T is measured in units of the crossing time between reflections and $v = \tanh\alpha$. Dissipation must be used to control such growth of short wavelength error.

It is instructive to interpret the boundary conditions on a wave in special relativity in the shifted coordinate system (2.3) where the boundary has fixed location but moves relative to the $t =$ const Cauchy hypersurfaces. In the 1D case, this gives rise to the half-plane problem

$$(\partial_t^2 - 2\beta\partial_x\partial_t - (1 - \beta^2)\partial_x^2)u = 0, \tag{2.10}$$

in the region $x \leq 0$ (where we now write $\beta^x = \beta$). There are two different frames in which the energy of the wave can be considered - the rest frame of the boundary and the rest frame intrinsic to the Cauchy hypersurfaces. In the rest frame of the boundary, the energy is

$$E = \frac{1}{2}\int_{-\infty}^{0} dx((\partial_t u)^2 + (1 - \beta^2)(\partial_x u)^2) \tag{2.11}$$

and satisfies

$$\partial_t E = \partial_t u((1 - \beta^2)\partial_x + \beta\partial_t)u|_{x=0}. \tag{2.12}$$

In the case $\beta^2 < 1$, this energy provides a norm and the semidiscrete version of the flux-conservation law (2.12) provides the basis for establishing stable evolution-boundary algorithms for the W-algorithm (1.8). Note the sign of β is important here in formulating a stable Neumann boundary condition. A homogeneous Neumann boundary condition takes the dissipative form

$$((1 - \beta^2)\partial_x + \beta\partial_t)u = 0. \tag{2.13}$$

The familiar form $\partial_x u = 0$ implies $\partial_t E \leq 0$ and thus guarantees a well-posed problem only when $\beta > 0$, i.e. only when the motion of the boundary is outward relative to the Cauchy hypersurfaces.

The energy intrinsic to the Cauchy hypersurfaces,

$$E_0 = \frac{1}{2}\int_{-\infty}^{0} dx((\partial_t u - \beta\partial_x u)^2 + (\partial_x u)^2), \tag{2.14}$$

provides a norm even in the superluminal case when $\beta^2 > 1$. It satisfies

$$\partial_t E_0 = \left(\frac{\beta}{2}(\partial_t u - \beta\partial_x u)^2 + \frac{\beta}{2}(\partial_x u)^2 + (\partial_t u - \beta\partial_x u)\partial_x u\right)\Big|_{x=0}. \tag{2.15}$$

Thus, in the absence of a boundary, (2.15) would reduce to $\partial_t E_0 = 0$ so that the Cauchy problem is well-posed for any β. The energy analogous to E_0 is used in Sec. III to establish well-posedness of the Cauchy problem and the stability of superluminal algorithms in the general multi-dimensional case.

When $\beta < -1$, i.e. when the motion of the boundary is superluminal and directed toward the Cauchy hypersurfaces, it is easy to verify that (2.15) implies $\partial_t E_0 < 0$ so that there is always a loss of energy through the boundary. This is the case of a spacelike boundary through which all the characteristics leave, i.e. a pure ''outflow'' boundary. Stable algorithms for such a boundary are also given in Sec. III for the higher dimensional case. Note that for $\beta > 1$ the boundary is also spacelike but now (2.15) implies $\partial_t E_0 > 0$. This is the pure ''inflow'' case, in which all the characteristics enter the boundary. This should not be considered in the context of an initial-boundary value problem, but as a pure Cauchy problem where the boundary represents a nonsmooth extension of the Cauchy hypersurface.

Further subtleties arise in treating co-orbiting, binary black holes. One strategy for the binary problem is to use a rotating coordinate system which co-orbits with the black holes. In the Schwarzschild case, the use of a coordinate $\varphi = \phi - \omega t$ rotating with angular velocity ω transforms the wave Eq. (2.6) into

$$\left(\left(1 + \frac{2M}{r}\right)(\partial_t + \omega\partial_\varphi)^2 - \frac{4M}{r}\partial_t\partial_r - \left(1 - \frac{2M}{r}\right)\partial_r^2 - \frac{1}{r^2}\left(\partial_\theta^2 + \frac{1}{\sin^2\theta}\partial_\varphi^2\right)\right)u = 0. \tag{2.16}$$

Now the t-direction becomes spacelike in the region

$$\left(1+\frac{2M}{r}\right)r^2\omega^2\sin^2\theta > 1, \tag{2.17}$$

which intersects the outer boundary $r = R_2$ if R_2 is sufficiently large. In that case, although the boundary remains timelike the evolution is superluminal so that the W-algorithm is no longer stable. A stable algorithm for such a boundary problem has been established in the 1D case [23]. We will not consider the 2D version of this problem here.

A common strategy for treating the binary black hole problem is to use a grid based upon Cartesian coordinates. This poses a problem in dealing with inner and outer boundaries with the spherical shapes natural to the problem. In other second order wave problems, such curved boundaries have been successfully treated by the embedded boundary method [19,25]. Another approach being explored in general relativity is to use multiblock grids [26–29]. This is another problem which we defer to future work and do not consider here.

III. ALGORITHMS FOR THE 2D SUPERLUMINAL PROBLEM

In this section, we study a class of second order hyperbolic systems with shift which we will use in Sec. V to construct stable algorithms for a model 2D black hole excision problem. The excision problem is a strip problem with spacelike and timelike boundaries and a horizon in between. In the region where the shift is superluminal, the boundary is spacelike and where the shift is subluminal, the boundary is timelike. We replace this problem by Cauchy and half-space problems. The strip problem is well-posed if the corresponding Cauchy and half-space problems are well-posed [30].

For the Cauchy problem, we consider general systems of equations in s space dimensions to demonstrate that the results have applicability beyond numerical relativity. For the half-space problems, we only consider scalar equations in 2D to simplify the notation. The generalization from scalar equations in 2D to systems in sD is quite straightforward.

Here, we consider systems with constant coefficients. Systems with variable coefficients can be reduced to systems with constant coefficients by freezing the coefficients at all points. The problem with variable coefficients is strongly well-posed if the Kreiss condition holds uniformly for all problems with constant coefficients [31].

In order to analyze and establish stable approximations we use the method of lines and reduce the system of partial differential equations to a system of ordinary differential equations in time on a spatial grid. We then apply two standard techniques: the energy method and mode analysis. The stability of the semidiscrete approximation implies the stability of the totally discretized method for most standard methods of lines [32], e.g. with the use of a Runge-Kutta time integrator.

A. The Cauchy problem

We consider the Cauchy problem for a second order system with constant (possibly complex) coefficients in s space dimensions,

$$\begin{aligned}\mathbf{u}_{tt} &= \sum_{j,k=1}^{s} A_{jk}\frac{\partial}{\partial\tilde{x}_j}\frac{\partial}{\partial\tilde{x}_k}\mathbf{u} := P_0(\partial/\partial\tilde{x})\mathbf{u},\\ \tilde{\mathbf{x}} &= (\tilde{x}_1,\ldots,\tilde{x}_s)\in\mathbb{R}^s, \qquad t\geq 0,\end{aligned} \tag{3.1}$$

with the initial conditions

$$\mathbf{u}(\tilde{\mathbf{x}}, t=0) = \mathbf{f}(\tilde{\mathbf{x}}), \quad \mathbf{u}_t(\tilde{\mathbf{x}}, t=0) = \mathbf{g}(\tilde{\mathbf{x}}), \quad \mathbf{u},\mathbf{f},\mathbf{g}\in\mathbb{C}^n. \tag{3.2}$$

(We abbreviate $\partial_\alpha u = u_\alpha$ where confusion does not arise.) Here, for each (j,k), A_{jk} are constant Hermitian matrices $\in\mathbb{C}^{n,n}$, and the data $\mathbf{f} = \mathbf{f}(\tilde{\mathbf{x}})$ and $\mathbf{g} = \mathbf{g}(\tilde{\mathbf{x}})$ are smooth and 1-periodic in each $\tilde{x}_j$, $j = 1,\ldots,s$. The solution $\mathbf{u} = \mathbf{u}(\tilde{\mathbf{x}}, t)$ is then smooth and 1-periodic in each $\tilde{x}_j$. Moreover, we consider solutions with $\int_{\mathbb{R}^s}\mathbf{u}\,d\tilde{\mathbf{x}} = 0$.

We assume that the Hermitian operator P_0 in (3.1) is elliptic, i. e. there exists a positive constant δ such that

$$\sum_{j,k=1}^{s} A_{jk}\xi_j\xi_k \geq \delta|\xi|^2 I \tag{3.3}$$

for all vectors $\xi\in\mathbb{R}^s$. Here I is the $n\times n$ identity matrix.

We introduce a shift by

$$\begin{aligned}\tilde{\mathbf{x}} &= \mathbf{x} + \bar{\beta}t, \qquad \mathbf{x} = (x_1,\ldots,x_s)\in\mathbb{R}^s,\\ \bar{\beta} &= (\beta^1,\ldots,\beta^s)\in\mathbb{R}^s, \qquad \beta^j > 0,\end{aligned}$$

and obtain the shifted system

$$\mathbf{u}_{tt} = 2P_1(\partial/\partial x)\mathbf{u}_t - P_1^2(\partial/\partial x)\mathbf{u} + P_0(\partial/\partial x)\mathbf{u}. \tag{3.4}$$

Here P_1 is a scalar operator,

$$P_1(\partial/\partial x) = \sum_{j=1}^{s}\beta^j\frac{\partial}{\partial x_j}.$$

Theorem 1.—The Cauchy problem for (3.4) is well-posed.

Proof.—If we set $\mathbf{v} = \mathbf{u}_t - P_1(\partial/\partial x)\mathbf{u}$, we get the first order system

$$\begin{pmatrix}\mathbf{u}\\ \mathbf{v}\end{pmatrix}_t = P_1(\partial/\partial x)\begin{pmatrix}\mathbf{u}\\ \mathbf{v}\end{pmatrix} + \begin{pmatrix}0 & I\\ P_0(\partial/\partial x) & 0\end{pmatrix}\begin{pmatrix}\mathbf{u}\\ \mathbf{v}\end{pmatrix}. \tag{3.5}$$

We Fourier transform (3.5) and get

$$\begin{pmatrix}\hat{\mathbf{u}}\\ \hat{\mathbf{v}}\end{pmatrix}_t = \hat{P}_1(i\omega)\begin{pmatrix}\hat{\mathbf{u}}\\ \hat{\mathbf{v}}\end{pmatrix} + \begin{pmatrix}0 & I\\ -\hat{P}_0(\omega) & 0\end{pmatrix}\begin{pmatrix}\hat{\mathbf{u}}\\ \hat{\mathbf{v}}\end{pmatrix}, \qquad \omega\neq\mathbf{0}, \tag{3.6}$$

where $\omega = (\omega_1,\ldots,\omega_s)\in\mathbb{R}^s$ and $\hat{P}_1(i\omega) = i\sum_{j=1}^{s}\beta^j\omega_j$

and $\hat{P}_0(\omega) = \sum_{j,k=1}^{s} A_{jk}\omega_j\omega_k$. Since P_0 is elliptic, we have $\hat{P}_0 = \hat{P}_0^* \geq \delta_0|\omega|^2 I$, for some $\delta_0 > 0$. We can then introduce new variables

$$\hat{\mathbf{w}} = T\begin{pmatrix} \hat{\mathbf{u}} \\ \hat{\mathbf{v}} \end{pmatrix}, \qquad T = \begin{pmatrix} I & 0 \\ 0 & \hat{P}_0^{-1/2} \end{pmatrix} \tag{3.7}$$

and, since T and $\hat{P}_1$ commute, we obtain from (3.6)

$$\hat{\mathbf{w}}_t = \hat{P}_1(i\omega)\hat{\mathbf{w}} + \begin{pmatrix} 0 & \hat{P}_0^{1/2}(\omega) \\ -\hat{P}_0^{1/2}(\omega) & 0 \end{pmatrix}\hat{\mathbf{w}} := S\hat{\mathbf{w}}. \tag{3.8}$$

Since the matrix S is skew Hermitian, $S^* = -S$, we obtain

$$\frac{\partial}{\partial t}||\hat{\mathbf{w}}||^2 = (S\hat{\mathbf{w}}, \hat{\mathbf{w}}) + (\hat{\mathbf{w}}, S\hat{\mathbf{w}}) = (\hat{\mathbf{w}}, (S^* + S)\hat{\mathbf{w}}) = 0.$$

Therefore, by Parseval's relation, there is an energy estimate and the Cauchy problem is well-posed [30].

Now we show how to construct stable finite difference approximations to (3.4). We leave time continuous and use the method of lines. For brevity, we treat the case $\beta^j > 0$.

Let $h_j = 1/N_j$, $j = 1, \ldots, s$, denote spatial gridlengths, where N_j are natural numbers. For any multi-index $\nu = (\nu_1, \ldots, \nu_s) \in \mathbb{Z}^s$, let $\mathbf{x}_\nu = (h_1\nu_1, \ldots, h_s\nu_s)$ denote the corresponding gridpoint. We consider gridfunctions $\mathbf{u}_\nu := \mathbf{u}_\nu(\mathbf{x}_\nu, t)$ approximating $\mathbf{u}(\mathbf{x}_\nu, t)$ and introduce a translation operator E_j in the j-th coordinate by

$$E_j^p\mathbf{u}_\nu = \mathbf{u}_\nu(\mathbf{x}_\nu + ph_j\mathbf{e}_j, t), \qquad p \in \mathbb{Z},$$

where $\mathbf{e}_j = (0, \ldots, 0, 1, 0, \ldots, 0)$ is the vector containing a 1 in the j-th position and zeros elsewhere. We then define the forward, backward, and the central difference operators in the j-th coordinate direction by

$$h_jD_{+j} = E_j^1 - E_j^0, \qquad h_jD_{-j} = E_j^0 - E_j^{-1},$$
$$2D_{0j} = D_{+j} + D_{-j}.$$

We approximate (3.4) by

$$\mathbf{u}_{\nu tt} = 2p_1(D)\mathbf{u}_{\nu t} - p_1^2(D)\mathbf{u}_\nu + p_0(D)\mathbf{u}_\nu, \tag{3.9}$$

where $p_0(D)$ is the centered approximation

$$p_0(D) = \sum_{j=1}^{s} A_{jj}D_{+j}D_{-j} + \sum_{j\neq k=1}^{s} A_{jk}D_{0j}D_{0k}, \tag{3.10}$$

and $p_1(D)$ is any one of the following approximations:

(1) Centered approximation,

$$p_1(D) = \sum_{j=1}^{s} \beta^j D_{0j}, \tag{3.11}$$

(2) First order accurate one-sided approximation,

$$p_1(D) = \sum_{j=1}^{s} \beta^j D_{+j}, \tag{3.12}$$

(3) Second order accurate one-sided approximation,

$$p_1(D) = \sum_{j=1}^{s} \beta^j D_{pj}, \tag{3.13}$$

where

$$D_{pj} = D_{+j} - \frac{h_j}{2}D_{+j}^2. \tag{3.14}$$

Remark.—It is not necessary to assume that $\beta^j > 0$ in (3.11), (3.12), and (3.13). In general, we can use $\frac{\beta^j+|\beta^j|}{2}D_{+j} + \frac{\beta^j-|\beta^j|}{2}D_{-j}$ in (3.12). For the second order one-sided approximation (3.13), we replace D_{+j} and D_{-j} by D_{pj} and $D_{mj} = D_{-j} + \frac{h_j}{2}D_{-j}^2$, respectively.

Theorem 2.—The approximation (3.9) is stable.

Proof.—As in the continuum case, we write (3.9) as a first order system and Fourier transform to get

$$\begin{pmatrix} \hat{\mathbf{u}} \\ \hat{\mathbf{v}} \end{pmatrix}_t = \hat{p}_1\begin{pmatrix} \hat{\mathbf{u}} \\ \hat{\mathbf{v}} \end{pmatrix} + \begin{pmatrix} 0 & I \\ -\hat{p}_0 & 0 \end{pmatrix}\begin{pmatrix} \hat{\mathbf{u}} \\ \hat{\mathbf{v}} \end{pmatrix}, \tag{3.15}$$

where

$$\hat{p}_0 = \sum_{j=1}^{s} A_{jj}\frac{4}{h_j^2}\sin^2\frac{\xi_j}{2} + \sum_{j\neq k=1}^{s} A_{jk}\frac{1}{h_jh_k}\sin\xi_j\sin\xi_k,$$
$$\xi_j = \omega_jh_j, \qquad |\xi_j| \leq \pi, \tag{3.16}$$

and $\hat{p}_1$ is one of the following:

$$\hat{p}_1 = \sum_{j=1}^{s} \beta^j\frac{1}{h_j}i\sin\xi_j, \tag{3.17}$$

$$\hat{p}_1 = \sum_{j=1}^{s} \beta^j\frac{1}{h_j}\left(i\sin\xi_j - 2\sin^2\frac{\xi_j}{2}\right), \tag{3.18}$$

$$\hat{p}_1 = \sum_{j=1}^{s} \beta^j\frac{1}{h_j}\left(i\sin\xi_j\left(1 - 2\sin^2\frac{\xi_j}{2}\right) - 4\sin^4\frac{\xi_j}{2}\right), \tag{3.19}$$

corresponding to (3.11), (3.12), and (3.13).

Since

$$\sin^2\xi = 4\sin^2\frac{\xi}{2}\cos^2\frac{\xi}{2} = 4\sin^2\frac{\xi}{2} - 4\sin^4\frac{\xi}{2}, \tag{3.20}$$

we have

$$\hat{p}_0 = \sum_{j,k=1}^{s} A_{jk} \frac{1}{h_j h_k} \sin\xi_j \sin\xi_k + \sum_{j=1}^{s} A_{jj} \frac{4}{h_j^2} \sin^4 \frac{\xi_j}{2}. \tag{3.21}$$

From the ellipticity condition (3.3) it follows that $\hat{p}_0$ is positive. As $\xi_j \to 0$ we have $\sin\xi_j/h_j \to \omega_j$. Therefore, the first sum in (3.21) is strictly positive. When $|\xi_j| = \pi$, the first sum in (3.21) is zero but the second sum is not because $\sin\frac{\xi_j}{2} \neq 0$. Therefore $\hat{p}_0$ is positive definite, and we can use the same transformation as in (3.7) and write (3.15) as

$$\hat{\mathbf{w}}_t = \hat{p}_1 \hat{\mathbf{w}} + \begin{pmatrix} 0 & \hat{p}_0^{1/2}(\omega) \\ -\hat{p}_0^{1/2}(\omega) & 0 \end{pmatrix} \hat{\mathbf{w}}. \tag{3.22}$$

The second term on the right hand side of (3.22) is again skew Hermitian and has no influence on the stability. Thus, we need only consider

$$\hat{\mathbf{w}}_t = \hat{p}_1 \hat{\mathbf{w}},$$

which consists of difference approximations of scalar equations of the above type. To show that the approximations (3.11), (3.12), and (3.13) are stable, we set $\hat{u} = e^{\lambda t}\hat{u}_0$ and get $\lambda = \hat{p}_1$. By (3.17), (3.18), and (3.19), we have $\Re\lambda \leq 0$ and there are no exponentially growing modes.

The approximation (3.9) involves a wide stencil. Therefore extra boundary conditions (ghost points) are required and the resulting accuracy is less than with a more compact stencil. In order to investigate other approximations with a more compact stencil, we write (3.4) as

$$\begin{aligned} \mathbf{u}_{tt} &= 2P_1(\partial/\partial x)\mathbf{u}_t + P(\partial/\partial x)\mathbf{u}, \\ P(\partial/\partial x) &= P_0(\partial/\partial x) - P_1^2(\partial/\partial x) \end{aligned} \tag{3.23}$$

and approximate it by

$$\mathbf{u}_{\nu tt} = 2p_1(D)\mathbf{u}_{\nu t} + p(D)\mathbf{u}_\nu, \tag{3.24}$$

where $p_1(D)$ is given by (3.11) and $p(D)$ is the centered approximation

$$p(D) = \sum_{j=1}^{s} (A_{jj} - \beta^{j2}) D_{+j} D_{-j} + \sum_{j\neq k=1}^{s} (A_{jk} - \beta^j \beta^k) D_{0j} D_{0k}. \tag{3.25}$$

Theorem 3.—The approximation (3.24) is stable if $A_{jj} - \beta^{j2} > 0$.

Proof.—We write (3.24) as

$$\begin{aligned} \mathbf{u}_{\nu tt} &= 2p_1(D)\mathbf{u}_{\nu t} - p_1^2(D)\mathbf{u}_\nu + q(D)\mathbf{u}_\nu, \\ q(D) &= p(D) + p_1^2(D). \end{aligned} \tag{3.26}$$

We use the relation $D_{+j}D_{-j} = D_{0j}^2 - \frac{h_j^2}{4} D_{+j}^2 D_{-j}^2$ and write

$$q(D) = \sum_{j,k=1}^{s} A_{jk} D_{0j} D_{0k} - \frac{1}{4} \sum_{j=1}^{s} (A_{jj} - \beta^{j2}) h_j^2 D_{+j}^2 D_{-j}^2.$$

In the same way as in the continuum case, we write (3.26) as a first order system and Fourier transform to get

$$\begin{pmatrix} \hat{\mathbf{u}} \\ \hat{\mathbf{v}} \end{pmatrix}_t = \hat{p}_1 \begin{pmatrix} \hat{\mathbf{u}} \\ \hat{\mathbf{v}} \end{pmatrix} + \begin{pmatrix} 0 & I \\ -\hat{q} & 0 \end{pmatrix} \begin{pmatrix} \hat{\mathbf{u}} \\ \hat{\mathbf{v}} \end{pmatrix}, \tag{3.27}$$

where

$$\begin{aligned} \hat{q} &= \sum_{j,k=1}^{s} A_{jk} \frac{1}{h_j h_k} \sin\xi_j \sin\xi_k + \sum_{j=1}^{s} (A_{jj} - \beta^{j2}) \frac{4}{h_j^2} \sin^4 \frac{\xi_j}{2}, \\ \xi_j &= \omega_j h_j, \qquad |\xi_j| \leq \pi \end{aligned} \tag{3.28}$$

and $\hat{p}_1$ is given by (3.17). By the ellipticity condition (3.3), it is clear that $\hat{q}$ is a positive definite matrix if $A_{jj} - \beta^{j2} > 0$. Therefore, we can use the same transformation as in (3.7) and write (3.27) as

$$\hat{\mathbf{w}}_t = \hat{p}_1 \hat{\mathbf{w}} + \begin{pmatrix} 0 & \hat{q}^{1/2}(\omega) \\ -\hat{q}^{1/2}(\omega) & 0 \end{pmatrix} \hat{\mathbf{w}}. \tag{3.29}$$

The second term on the right hand side of (3.29) is again skew Hermitian and has no influence on the stability. Thus, we need only to consider

$$\hat{\mathbf{w}}_t = \hat{p}_1 \hat{\mathbf{w}},$$

and the stability follows in the same way as in Theorem 2.

Remark.—If the operator P is elliptic, we have $A_{jj} - \beta^{j2} > 0$, and by Theorem 3 the approximation (3.24) is stable. However, it is possible to have $A_{jj} - \beta^{j2} > 0$ while P is nonelliptic. In this case, the approximation (3.24) remains stable when P is nonelliptic. In other words, the stability of (3.24) does not depend upon the coefficients of mixed derivatives A_{jk}, $j \neq k$.

Remark.—In the scalar case, (3.24) reduces to the W-algorithm (1.8).

In the excision problem, we use the subluminal algorithm (3.24) in the subluminal region where $A_{jj} - \beta^{j2} > 0$. In the superluminal region where the shift β^j is large so that $A_{jj} - \beta^{j2} \leq 0$, we use the superluminal algorithm (3.9) instead. We need then a prescription for switching from one algorithm to the other. There are two distinct ways to do this. One is to make a sharp switch between the algorithms where the transition from superluminal to subluminal region takes place. The other, used in [13], is to introduce a smooth, monotonic blending function and use a blended algorithm, which turns into the superluminal algorithm inside the superluminal region and reduces monotonically to the subluminal algorithm in the outside. For this purpose, note that the superluminal algorithm remains stable in the subluminal region.

As a further alternative to the above approximations, we can approximate (3.23) by adding a fourth differential order term

$$\mathbf{u}_{\nu tt} = 2p_1(D)\mathbf{u}_{\nu t} + p(D)\mathbf{u}_\nu - Q(D)\mathbf{u}_\nu, \qquad (3.30)$$

where $p_1(D)$ is given by (3.11) and

$$Q(D) = \frac{1}{4}\sum_{j=1}^{s} \alpha_j h_j^2 D_{+j}^2 D_{-j}^2, \qquad \alpha_j \geq 0. \qquad (3.31)$$

The motivation for adding such a fourth order term is to modify the matrix $\hat{q}$ in (3.28) so that it becomes positive definite even if $A_{jj} - \beta^{j2} \leq 0$. When $A_{jj} - \beta^{j2} > 0$, the matrix $\hat{q}$ is positive definite and this added term is unnecessary. We can take advantage of this by embedding the switch or blending function in the choice of α_j, with $\alpha_j = 0$ in the outer region.

Theorem 4.—The approximation (3.30) is stable if $A_{jj} + \alpha_j I \geq \beta^{j2} I$.

Proof.—We use the relation $D_{0j}^2 = D_{+j}D_{-j} + \frac{h_j^2}{4} D_{+j}^2 D_{-j}^2$ and write

$$\begin{aligned} p(D) &= \sum_{j,k=1}^{s} (A_{jk} - \beta^j \beta^k) D_{0j} D_{0k} \\ &\quad - \frac{1}{4}\sum_{j=1}^{s} (A_{jj} - \beta^{j2}) h_j^2 D_{+j}^2 D_{-j}^2 \\ &= -p_1^2(D) + \sum_{j,k=1}^{s} A_{jk} D_{0j} D_{0k} \\ &\quad - \frac{1}{4}\sum_{j=1}^{s} (A_{jj} - \beta^{j2}) h_j^2 D_{+j}^2 D_{-j}^2. \end{aligned}$$

We can then write (3.30) as

$$\mathbf{u}_{\nu tt} = 2p_1(D)\mathbf{u}_{\nu t} - p_1^2(D)\mathbf{u}_\nu + q(D)\mathbf{u}_\nu, \qquad (3.32)$$

where

$$\begin{aligned} q(D) &= \sum_{j,k=1}^{s} A_{jk} D_{0j} D_{0k} \\ &\quad - \frac{1}{4}\sum_{j=1}^{s} (A_{jj} - \beta^{j2} + \alpha_j) h_j^2 D_{+j}^2 D_{-j}^2. \end{aligned} \qquad (3.33)$$

In the same way as before, we write (3.33) as a first order system and Fourier transform to get

$$\begin{pmatrix} \hat{\mathbf{u}} \\ \hat{\mathbf{v}} \end{pmatrix}_t = \hat{p}_1 \begin{pmatrix} \hat{\mathbf{u}} \\ \hat{\mathbf{v}} \end{pmatrix} + \begin{pmatrix} 0 & I \\ -\hat{q} & 0 \end{pmatrix} \begin{pmatrix} \hat{\mathbf{u}} \\ \hat{\mathbf{v}} \end{pmatrix}, \qquad (3.34)$$

where

$$\begin{aligned} \hat{q} &= \sum_{j,k=1}^{s} A_{jk} \frac{1}{h_j h_k} \sin\xi_j \sin\xi_k \\ &\quad + \sum_{j=1}^{s} (A_{jj} - \beta^{j2} + \alpha_j) \frac{4}{h_j^2} \sin^4 \frac{\xi_j}{2}. \end{aligned}$$

If $A_{jj} + \alpha_j I \geq \beta^{j2} I$ then, because of ellipticity, $\hat{q}$ is positive definite and stability follows in the same way as before.

B. Half-plane problems

We consider the scalar wave equation with constant coefficients in two space dimensions,

$$u_{\tilde{t}\tilde{t}} = a_1 u_{\tilde{x}\tilde{x}} + 2b_1 u_{\tilde{x}\tilde{y}} + c_1 u_{\tilde{y}\tilde{y}} := P_0 u. \qquad (3.35)$$

In the moving coordinate system, $t = \tilde{t}$, $x = \tilde{x} - \beta^x \tilde{t}$, $y = \tilde{y} - \beta^y \tilde{t}$, with $\beta^x, \beta^y > 0$, we get the shifted wave equation,

$$\begin{aligned} u_{tt} &= 2(\beta^x u_{xt} + \beta^y u_{yt}) + a u_{xx} + 2b u_{xy} + c u_{yy} \\ &:= 2P_1 u_t + Pu. \end{aligned} \qquad (3.36)$$

Here the coefficients $a = a_1 - \beta^{x2}$, $b = b_1 - \beta^x \beta^y$, and $c = c_1 - \beta^{x2}$ are assumed to be constant. Moreover, we assume that the space operator P_0 in (3.36) is elliptic, namely $a_1 > 0$ and $c_1 > 0$ and $b_1^2 < a_1 c_1$. Therefore, by Theorem 1, the Cauchy problem for (3.36) is well-posed.

We consider (3.36) in the half-space

$$0 \leq x < \infty, \qquad -\infty < y < \infty, \qquad t \geq 0$$

and we assume that u is 1-periodic in y. The number of boundary conditions needed at $x = 0$ is equal to the number of outgoing characteristics of the equation $u_{tt} = 2\beta^x u_{xt} + a u_{xx}$. We consider two distinct half-plane problems determined by the coefficients of the operator P.

Half-plane problem I: If $a > 0$ and $b^2 < ac$, then the operator P is elliptic and one boundary condition is needed at $x = 0$. In the excision problem, this is the case of subluminal shift with a timelike boundary.

Half-plane problem II: If $a < 0$, then the operator P is nonelliptic. In the excision problem, this is the case of a superluminal shift with a spacelike boundary.

1. Half-plane problem I (subluminal case)

This is the problem treated in [12] by the energy method. In the present context of (3.36), the energy is given by

$$E = \|u_t\|^2 + a\|u_x\|^2 + 2b(u_x, u_y) + c\|u_y\|^2 \qquad (3.37)$$

in terms of the L_2 scalar product and the corresponding norm

$$(v, w) = \int_0^1 \int_0^\infty v w dx dy, \qquad \|v\|^2 = (v, v). \qquad (3.38)$$

If u solves (3.36), then integration by parts gives

$$\partial_t E = -2u_t(\beta^x u_t + a u_x + b u_y)|_{x=0}. \tag{3.39}$$

Any boundary condition satisfying the dissipative condition $\partial_t E \le 0$ gives an energy estimate sufficient to establish the well-posedness of the Cauchy problem, including the Dirichlet condition

$$u_t(0, y, t) = 0 \tag{3.40}$$

and the Neumann condition

$$\beta^x u_t(0, y, t) + a u_x(0, y, t) + b u_y(0, y, t) = 0 \tag{3.41}$$

for which energy is conserved.

As difference approximation for the half-plane problem, we use (3.24), which in the present case reduces to the W-algorithm (1.8). By introducing a discrete energy norm and using summation by parts, a discrete version of (3.39) has been used to establish stability of the finite difference problem. For details we refer to [12].

2. Half-plane problem II (superluminal case)

To investigate the well-posedness of the continuum problem, we use mode analysis. We apply a Laplace transformation in t and Fourier transformation in y.

Theorem 5.—The half-plane problem (3.36) with $a < 0$ is well-posed.

Proof.—By substituting $u = \hat{u}(x)e^{st+i\omega y}$, $s \in \mathbb{C}$, $\omega \in \mathbb{R}$, into (3.36) we obtain

$$a\hat{u}_{xx} + (2ib\omega + 2\beta^x s)\hat{u}_x + (2i\beta^y \omega s - s^2 - c\omega^2)\hat{u} = 0. \tag{3.42}$$

The general solution to the ordinary differential Eq. (3.42) is of the form $\hat{u}(x) = \sigma_1 e^{\kappa_1 x} + \sigma_2 e^{\kappa_2 x}$, where κ_1 and κ_2 are the solutions of the characteristic equation

$$a\kappa^2 + (2bi\omega + 2\beta^x s)\kappa + 2i\beta^y \omega s - s^2 - c\omega^2 = 0. \tag{3.43}$$

Without restriction we can assume $a = -1$. Moreover, since the sign of $\Re\kappa$ does not depend on ω, we set $\omega = 0$. We then obtain

$$\kappa_{1,2} = \beta^x s \pm \sqrt{(\beta^{x2} - 1)s^2}.$$

For $\Re s > 0$, we have $\Re\kappa_{1,2} > 0$ and there is no bounded solution $\hat{u}$. Therefore no boundary condition is needed and the problem is well-posed.

As difference approximation for the half-plane problem, we can use either (3.9) or (3.30). We study the stability of the approximations by mode analysis. Below we show that (3.9) is stable with $p_1(D)$ in (3.12). The stability of the other approximations with $p_1(D)$ in (3.11) and (3.13) can be shown in the same way.

On a uniform spatial grid $\Omega_h = (\nu h, \mu h)$, $\nu = 0, 1, 2, \ldots$, $\mu = 1, 2, \ldots, N$, with spacing h, let $v(t) := u_{\nu\mu}(t)$ be the gridfunction approximating $u(x_\nu, y_\mu, t)$. We consider the shifted wave Eq. (3.36) and approximate it by

$$v_{tt} = 2(\beta^x D_{+x} + \beta^y D_{+y})v_t - (\beta^x D_{+x} + \beta^y D_{+y})^2 v + (a_1 D_{+x} D_{-x} + 2b_1 D_{0x} D_{0y} + c_1 D_{+y} D_{-y})v, \tag{3.44}$$

for $\nu = 1, 2, \ldots$. For every fixed μ, we need one extra boundary condition to determine $u_{0\mu}$. We use a third order extrapolation

$$h^3 D_{+x}^3 u_{0\mu} = 0. \tag{3.45}$$

We consider bounded solutions of type

$$u_{\nu\mu}(t) = e^{st+i\omega\mu h}\varphi_\nu, \qquad \|\varphi\|_h < \infty. \tag{3.46}$$

Putting (3.46) into (3.44), we get the eigenvalue problem

$$\begin{aligned}
&\varphi_\nu s^2 - 2\frac{\beta^x}{h}(\varphi_{\nu+1} - \varphi_\nu)s - 2\frac{\beta^y}{h}\left(i\sin\xi - 2\sin^2\frac{\xi}{2}\right)\varphi_\nu s \\
&\quad + \frac{\beta^{x^2}}{h^2}(\varphi_{\nu+2} - 2\varphi_{\nu+1} + \varphi_\nu) + 2\frac{\beta^x\beta^y}{h^2}(\varphi_{\nu+1} - \varphi_\nu) \\
&\quad \times \left(i\sin\xi - 2\sin^2\frac{\xi}{2}\right) + \frac{\beta^{y^2}}{h^2}\left(i\sin^2\xi - 2\sin^2\frac{\xi}{2}\right)^2\varphi_\nu \\
&\quad - \frac{a_1}{h^2}(\varphi_{\nu+1} - 2\varphi_\nu + \varphi_{\nu-1}) - \frac{b_1}{h^2}i\sin\xi(\varphi_{\nu+1} - \varphi_{\nu-1}) \\
&\quad + 4\frac{c_1}{h^2}\sin^2\frac{\xi}{2}\varphi_\nu = 0, \qquad \xi = \omega h.
\end{aligned} \tag{3.47}$$

The approximation (3.44) and (3.45) is stable if and only if the Kreiss condition is satisfied, or equivalently if (3.47) has no eigenvalue s with $\Re s \ge 0$ [31]. The constant-coefficient ordinary difference Eq. (3.47) has solution of the form

$$\varphi_\nu = \sum_{j=1}^{3} \sigma_j \kappa_j^\nu,$$

where κ_j are the three solutions of the characteristic equation

$$\begin{aligned}
&s^2 - 2\left(\frac{\beta^x}{h}(\kappa - 1) + \frac{\beta^y}{h}\left(i\sin\xi - 2\sin^2\frac{\xi}{2}\right)\right)s \\
&\quad + \left(\frac{\beta^x}{h}(\kappa - 1) + \frac{\beta^y}{h}\left(i\sin\xi - 2\sin^2\frac{\xi}{2}\right)\right)^2 \\
&\quad - \frac{a_1}{h^2}\frac{(\kappa - 1)^2}{\kappa} - \frac{b_1}{h^2}\left(\kappa - \frac{1}{\kappa}\right)i\sin\xi + 4\frac{c_1}{h^2}\sin^2\frac{\xi}{2} = 0.
\end{aligned} \tag{3.48}$$

By Lemma 12.1.6 of [31], for $\Re s > 0$ the characteristic Eq. (3.48) has no solutions with $|\kappa| = 1$ and there is exactly one solution with $|\kappa| < 1$. Roughly speaking, the number of left points in the difference stencil determines the number of solutions to the characteristic equation with $|\kappa| < 1$. We call this solution κ_1 and write the bounded solution as

$$u_\nu(t) = e^{st+i\omega\mu h}\sigma_1\kappa_1^\nu. \tag{3.49}$$

By substituting (3.49) into the boundary condition (3.46), we get

$$\sigma_1(\kappa_1 - 1)^3 e^{st+i\omega\mu h} = 0. \tag{3.50}$$

Since $\kappa_1 \neq 1$ for $\Re s > 0$, (3.50) has only the trivial solution $\sigma_1 = 0$. Now, we let $\kappa \to 1$ and investigate if there is any sequence $\{s\}$ such that $\Re s \to 0$ with $\Re s > 0$. We then get from (3.48)

$$\tilde{s}^2 - 2\beta^y\left(i\sin\xi - 2\sin^2\frac{\xi}{2}\right)\tilde{s} + \beta^{y2}\left(i\sin\xi - 2\sin^2\frac{\xi}{2}\right)^2 + 4c_1\sin^2\frac{\xi}{2} = 0, \qquad \tilde{s} = sh, \tag{3.51}$$

and therefore

$$\tilde{s} = \beta^y\left(i\sin\xi - 2\sin^2\frac{\xi}{2}\right) \pm \sqrt{-4c_1\sin^2\frac{\xi}{2}}. \tag{3.52}$$

Since $\beta^y > 0$ and $c_1 > 0$, we have $\Re s < 0$ if $\xi \not\to 0$. In the case where $\xi \to 0$, we get from (3.48)

$$s^2 - 2\frac{\beta^x}{h}s(\kappa - 1) + \frac{\beta^{x2}}{h^2}(\kappa - 1)^2 - \frac{a_1}{h^2}\frac{(\kappa - 1)^2}{\kappa} = 0. \tag{3.53}$$

Letting $s \to 0$, we then get from (3.53) that $\kappa_{1,2} = 1$ and $\kappa_3 = a_1/\beta^{x2} < 1$. Since for $\Re s > 0$ there is no solution with $|\kappa| = 1$, the only solution is κ_3 which is strictly less than 1 and does not converge to 1. Therefore there is no positive sequence $\{s\}$ such that $\Re s \to 0$ for $|\xi| \leq \pi$. Now, we can prove the following theorem:

Theorem 6.—The approximation (3.44) and (3.45) is stable.

Proof.—Since there is no eigenvalue s with $\Re s \geq 0$ to the eigenvalue problem (3.47) giving bounded solutions (3.46), the Kreiss condition is satisfied and stability follows.

IV. TESTS OF THE SUPERLUMINAL ALGORITHMS

In the subluminal case where the evolution proceeds in a timelike direction, the W-algorithm (1.8) provides an accurate, flux-conservative, second order treatment of the IBVP. This was proved for a 1D quasilinear wave equation in [13] using the discrete energy method. In [10,12], the results were extended to the 3D case and applied to the harmonic Einstein system (1.2). The semidiscrete conservation laws extend to the principal part of the harmonic Einstein system and contribute to excellent long term performance in test problems. We use this W-algorithm to treat the outer region of the model excision problem considered in Sec. V.

In this model problem, the inner boundary is chosen to be spacelike, corresponding to the strategy for excising an interior singularity. The evolution near the inner boundary proceeds in a spacelike direction (superluminal shift) so that the spatial grid tracks the boundary. For this superluminal case, the W-algorithm is unstable and one of the algorithms considered in Sec. III must be used. These algorithms are either given by (3.9), with $p_1(D)$ given by one of the approximations (3.11), (3.12), and (3.13), or by (3.30).

In the case of the 2D shifted wave Eq. (1.6), the choice (3.11) reduces to the centered algorithm

$$V := ((\partial_t - \beta^x D_{0x} - \beta^y D_{0y})^2 - a_1 D_{+x}D_{-x} - c_1 D_{+y}D_{-y} - 2b_1 D_{0x}D_{0y})u = 0; \tag{4.1}$$

the choice (3.12) reduces to

$$V_+ := ((\partial_t - \beta^x D_{+x} - \beta^y D_{+y})^2 - a_1 D_{+x}D_{-x} - c_1 D_{+y}D_{-y} - 2b_1 D_{0x}D_{0y})u = 0, \tag{4.2}$$

in which the shift terms are treated by first order accurate one-sided difference operators; the choice (3.13) reduces to

$$V_p := ((\partial_t - \beta^x D_{px} - \beta^y D_{py})^2 - a_1 D_{+x}D_{-x} - c_1 D_{+y}D_{-y} - 2b_1 D_{0x}D_{0y})u = 0, \tag{4.3}$$

in which the shift terms are treated by second order accurate one-sided difference operators (3.14); and (3.30) is related to the subluminal W-algorithm (1.8) by

$$V_\alpha := W + \frac{h^2}{4}(\alpha_1(D_{+x}D_{-x})^2 + \alpha_2(D_{+y}D_{-y})^2)u = 0, \tag{4.4}$$

where Theorem 4 guarantees stability provided the inequalities

$$\alpha_1 \geq \beta^{x^2} - a_1 = -a, \qquad \alpha_1 \geq 0, \tag{4.5}$$

$$\alpha_2 \geq \beta^{y^2} - c_1 = -c, \qquad \alpha_2 \geq 0, \tag{4.6}$$

are satisfied.

The V-algorithm is related to the W-algorithm by the second order accurate modification

$$V = W + \frac{h^2}{4}(\beta^{x^2}(D_{+x}D_{-x})^2 + \beta^{y^2}(D_{+y}D_{-y})^2)u = 0. \tag{4.7}$$

In the subluminal case where the W and V algorithms can be compared, tests show that the W-algorithm has considerably better accuracy due to its more compact stencil [10]. Here we carry out a set of 2D superluminal tests to compare the performance of the superluminal algorithms in a periodic test problem (smooth toroidal boundary conditions) where the effect of the boundary is eliminated. The first order accurate V_+-algorithm (4.2) is highly dissipative and much less accurate than the second order accurate V_p version (4.3). For these reasons, we restrict our test comparisons to the V, V_p and V_α algorithms.

The V-algorithm is a special case of the V_α-algorithm (4.4) where $\alpha_1 = \beta^{x^2}$ and $\alpha_2 = \beta^{y^2}$. The accuracy of the V_α-algorithm might be expected to depend on the relative

weight of the higher order terms responsible for the stretched stencil in (4.4). For example, the V_α-algorithm might be expected to be most accurate for the minimum values, $\alpha_1 = (|a| - a)/2$ and $\alpha_2 = (|c| - c)/2$, which are allowed by (4.5) and (4.6). This is true for the case when a and c are positive, for which $\alpha_1 = \alpha_2 = 0$ and the V_α-algorithm reduces to the W-algorithm.

When $a < 0$ is negative and $c > 0$, the optimal value for α_2 remains 0 but the optimal value for α_1 is not necessarily the minimum allowed value $\alpha_1 = -a$. This value would result in approximating the $a\partial_x^2$ term in the wave operator by aD_{0x}^2, which decouples the even and odd grid points. Although the optimal choice of α_1 in this case is not obvious, the combination $\alpha_1 = \beta^{x^2}$ and $\alpha_2 = 0$ would give better accuracy than the V-algorithm. No general guidelines are suggested by examining the truncation error in the V_α-algorithm, which to order h^2 is given by

$$\tau = \frac{h^2}{12}((a - 3\alpha_1)\partial_x^4 + (c - 3\alpha_2)\partial_y^4 + 4b(\partial_x^3\partial_y + \partial_x\partial_y^3) + 4\beta^x\partial_x^3\partial_t + 4\beta^x\partial_y^3\partial_t)u. \quad (4.8)$$

Note that the values $\alpha_1 = a/3$ and $\alpha_2 = c/3$ correspond to the fourth order accurate approximations to the terms $a\partial_x^2$ and $c\partial_y^2$ in the wave operator. However, these choices are not allowed in the superluminal regime, where stability requires $\alpha_i \geq 0$.

As a test problem for comparing the accuracy of these evolution algorithms in the superluminal regime we pick a case where both a and c are negative. We consider the wave equation

$$(-\partial_t^2 + 4(\partial_x + \partial_y)\partial_t - 3\partial_x^2 - 3\partial_y^2 - 8\partial_x\partial_y)u = 0. \quad (4.9)$$

which arises from a 2D version of (2.4) with shift $\beta^x = \beta^y = 2$. With this superluminal choice of shift, there are no characteristics in the $(x > 0, y > 0)$ directions. Waves propagating along the diagonal have the form

$$u = F[x + y + (4 + \sqrt{2})t] + G[x + y + (4 - \sqrt{2})t]. \quad (4.10)$$

In our test, we simulate the solution

$$u = \sin(2\pi[x + y + (4 + \sqrt{2})t]) \quad (4.11)$$

in the domain $-.5 \leq (x, y) \leq .5$, on a grid with $N = 200$ points, with periodic boundary conditions. For this particular solution, the symmetries $\partial_x u = \partial_y u = \partial_t u/(4 + \sqrt{2})$ imply that the truncation error (4.8) has a minimum at $\alpha_1 = \alpha_2 = \alpha_m$, where

$$\alpha_m = \frac{13 + 8\sqrt{2}}{3} \approx 8.104\,569\,5. \quad (4.12)$$

Figure 1 plots the ℓ_∞ norm of the numerical error in the scalar field obtained in the simulation of (4.11) by evolving the wave Eq. (4.9) with the V_α-algorithm, for various values of $\alpha_1 = \alpha_2 = \alpha$. The error for $\alpha = 8.104\,569\,5$ is extremely small and the plots confirm that α_m is indeed the optimal value. The value $\alpha = 4$ corresponds to the V-algorithm, which gives significantly larger error. The value $\alpha = 3$, which is the smallest value allowed by stability, gives even larger error.

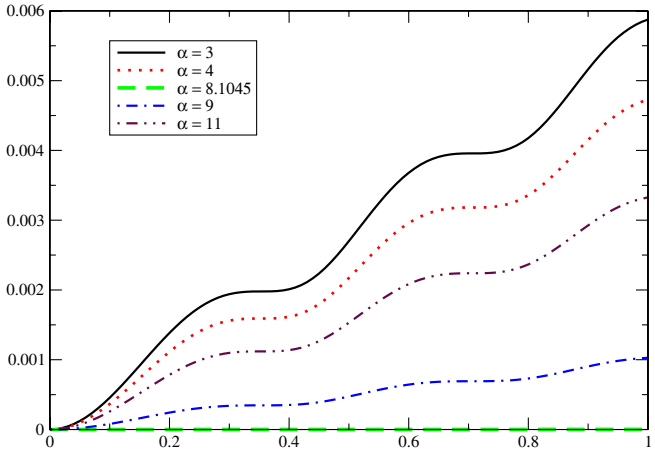

FIG. 1 (color online). The ℓ_∞ norm of the error of the scalar field obtained with V_α algorithm on a grid of 200 points is plotted vs time, in the interval $0 \leq t \leq 1$. For the value $\alpha_m \approx 8.104\,569\,5$, the error is barely discernible and the plots clearly indicate that α_m is the optimal value. The value $\alpha = 4$ corresponds to the V-algorithm, which has significantly larger error.

The error in Fig. 1 is predominantly phase error. Figure 2 shows snapshots of $u(t = 100, x)$ (100 crossing times) for the simulation of (4.11) using the V, V_p and V_α algorithms, with $\alpha = 8$. The simulations are compared with the analytical solution at $t = 100$. The solution with the V_p-algorithm leads in phase while that with the V-algorithm lags in phase and it has slightly better accuracy. As ex-

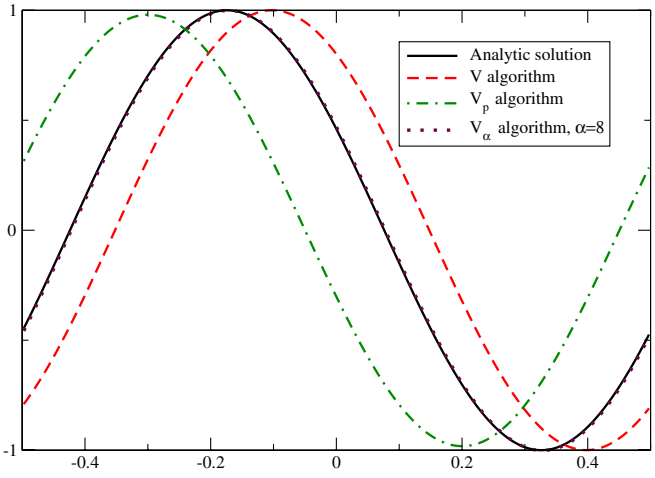

FIG. 2 (color online). Snapshots of the scalar field $u(t = 100, x)$ obtained with the V, V_p and V_α algorithms, compared with the analytic solution. The phase error with the V_p-algorithm is larger than with the V-algorithm. The V_α-algorithm, for $\alpha = 8$, is extremely accurate and barely distinguishable from the analytic solution.

pected from the above error analysis, the V_α-algorithm, with $\alpha = 8$, is extremely accurate.

V. SIMULATION OF A MODEL 2D EXCISION PROBLEM

In this section, we simulate a simple 2D model of the excision problem in which the inner boundary $\mathcal{S}$ is spacelike and the outer boundary $\mathcal{T}$ is timelike, with a horizon $\mathcal{H}$ in between. In the inner region between $\mathcal{S}$ and $\mathcal{H}$, since the shift is superluminal, the operator P in (3.23) is nonelliptic and both characteristics leave the inner boundary. In the outer region between $\mathcal{H}$ and $\mathcal{T}$, since the shift is subluminal, the operator P is elliptic and one characteristic leaves $\mathcal{T}$ and the other enters $\mathcal{T}$.

To model a wave pulse propagating into a horizon, we consider the shifted wave equation with a source term F,

$$u_{tt} = 2(\beta^x u_{xt} + \beta^y u_{yt}) + a u_{xx} + 2b u_{xy} + c u_{yy} + F(x, y, t), \tag{5.1}$$

on the spatial domain $(x, y) \in \Omega = [-2, 2] \times [-2, 2]$, and $t \geq 0$. We set the coefficients $\beta^x = \beta^y = 2$, $a = 0.5(x - \sin\frac{\pi y}{2})$, $b = 0.5$ and $c = 5$, for which the problem is well-posed. The spacelike boundary $\mathcal{S}$ at $x = -2$, the timelike boundary $\mathcal{T}$ at $x = 2$ and the horizon $\mathcal{H}$ are shown in Fig. 3. The horizon satisfies $ac - b^2 = 0$, which determines the curve

$$x = 0.1 + \sin\frac{\pi y}{2}. \tag{5.2}$$

For the smooth function

$$F(x, y, t) = \frac{2}{\sigma^2}(-(1 - 2\beta^x - a)(\sigma - 2(t + x - x_0)^2) - 4(\beta^y + b)(t + x - x_0)y + c(\sigma - 2y^2))e^{-((t+x-x_0)^2+y^2)/\sigma}, \tag{5.3}$$

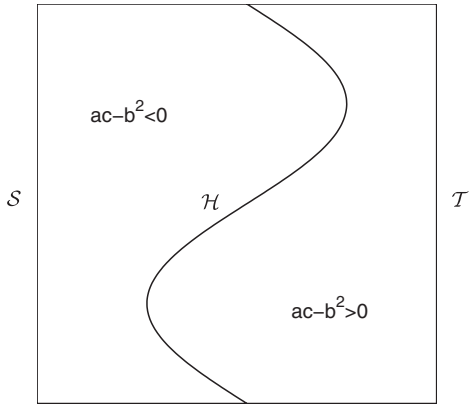

FIG. 3. Computational domain with the spacelike boundary $\mathcal{S}$ on the left, the timelike boundary $\mathcal{T}$ on the right and the sinusoidal shaped horizon $\mathcal{H}$ in between. The solution is periodic in the vertical y-direction.

the Eq. (5.1) has the solution

$$u(x, y, t) = e^{-((t+x-x_0)^2+y^2)/\sigma}, \tag{5.4}$$

which is a left-traveling wave packet, initially centered about $x_0 = 0.5$ outside the horizon and propagating towards the spacelike boundary. Here we set $\sigma = 0.05$. We uniformly discretize the spatial domain as $x_\nu = \nu h$ and $y_\mu = \mu h$ with $\nu, \mu = 0, \pm 1, \ldots, \pm N$ with the grid size $h = \frac{2}{N}$.

The global simulation of the model problem in the region between $\mathcal{S}$ and $\mathcal{T}$ is carried out by combining the superluminal V-algorithms established in Sec. III with the subluminal W-algorithm. The spacelike boundary and the superluminal region are treated with one of the V-algorithms. A region containing the timelike boundary is treated by the W-algorithm.

We consider the following three global algorithms:

(i) *Algorithm 1.*—The superluminal region is treated by the V-algorithm (4.3). In the subluminal region we use the W-algorithm. We introduce a cutoff function ϕ which is 0 when $a > 0$ and $c > 0$ and is 1 when $a \leq 0$ or $c \leq 0$. Then we use the following approximation

$$\phi V + (1 - \phi)W = 0.$$

(ii) *Algorithm 2.*—This is similar to **1**, except the superluminal region is treated by the V_p-algorithm (4.3), which is then blended to the W-algorithm in the same way as in **1**.

(iii) *Algorithm 3.*—We use the V_α-algorithm (4.4) with $\alpha_1 = (|a| - a)/2$ and $\alpha_2 = (|c| - c)/2$.

The initial data and boundary condition at $x = 2$ are chosen according to the exact solution (5.4). In the first and third algorithms, we need two extra boundary conditions at $\nu = -N, -N + 1$. In the second algorithm, we need only one boundary condition at $\nu = -N$. We use third order extrapolations as the extra boundary conditions. In the y-direction we use periodic boundary conditions. For the integration in time, we use the standard 4th order Runge-Kutta method.

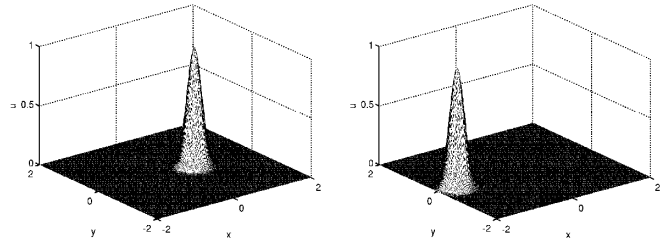

(a) The initial wave pulse at $t = 0$. (b) The wave pulse at $t = 2$.

FIG. 4. A pulse propagating across the horizon. The left figure shows the initial pulse in the region outside the horizon. The right figure shows the pulse at a later time, after it has crossed the horizon and is incident on the inner spacelike boundary.

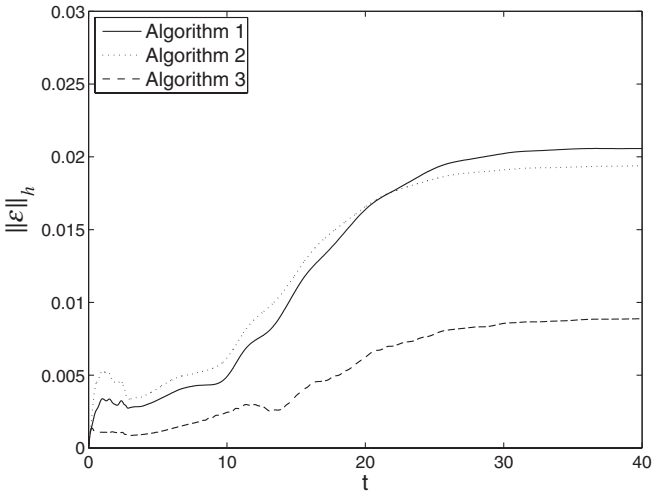

FIG. 5. Norm of the error $\|\mathcal{E}\|_h$ versus time, with $h = 0.02$.

Figure 4 shows the initial wave pulse and the pulse at a later time $t = 2$ computed by the third algorithm.

For the gridfunction $u_{\nu\mu}(t)$ approximating $u(x_\nu, y_\mu, t)$, we define the discrete norm as

$$\|u_{\nu\mu}\|_h^2 = \sum_{\nu,\mu=-N}^{N} u_{\nu\mu} h^2, \tag{5.5}$$

where $h = \Delta x = \Delta y$ is the gridlength. We then define the convergence factor by

$$\mathcal{C}(t) = \log_2\left(\frac{\|\mathcal{E}(t)\|_h}{\|\mathcal{E}(t)\|_{h/2}}\right), \qquad \mathcal{E}(t) = u(x_\nu, y_\mu, t) - u_{\nu\mu}(t), \tag{5.6}$$

where $\mathcal{E}(t)$ is the error at time t, and $u(x_\nu, y_\mu, t)$ is the exact solution computed by (5.4).

Figure 5 shows the norm of the error versus time for the three algorithms with $h = 0.02$ and $\Delta t = 0.001$.

Figure 6 shows the convergence factor as a function of time for the three algorithms with $h = 0.04$ and $\Delta t = 0.001$. It confirms the second order accuracy of the algorithms in space. The jumps in the convergence factor at about $t = 2$ is a result of using third order extrapolations at the spacelike inner boundary, while we use second order evolution algorithms. At this time the pulse reaches the spacelike boundary and an increase in the order of accuracy, from 2 to 3, is expected.

The third algorithm gives a better accuracy than the other two. The second algorithm, in which we use the second order one-sided stencil with extrapolation in one ghost point, gives a slightly smaller error than the first algorithm, in which the second order centered stencil with extrapolation in two ghost points is used.

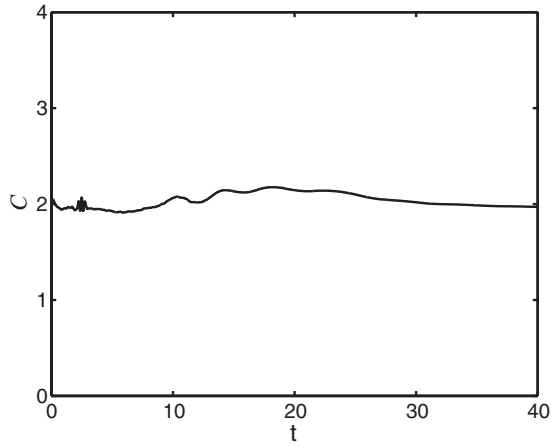

(a) Algorithm 1.

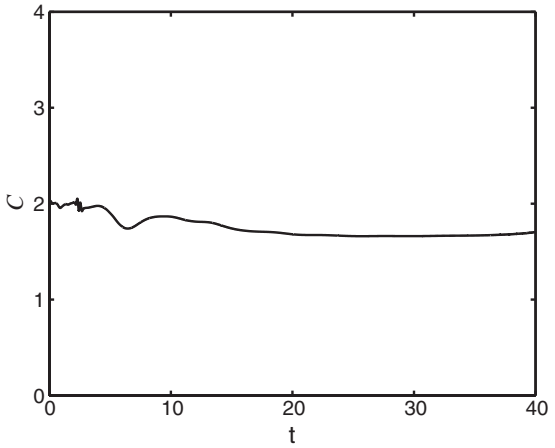

(b) Algorithm 2.

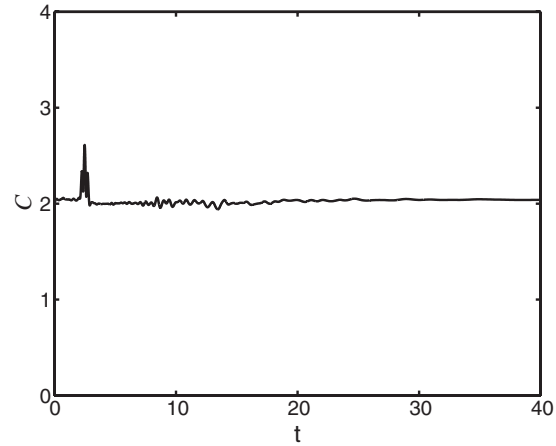

(c) Algorithm 3.

FIG. 6. Convergence factor $\mathcal{C}$ versus time indicates that the algorithms are second order accurate in space.

ACKNOWLEDGMENTS

This work was supported by the National Science Foundation under Grant No. PH-0244673 to the University of Pittsburgh. We have used computing resources of the Pittsburgh Supercomputing Center and of the National Energy Research Scientific Computing Center; and we have benefited from the use of the Cactus Computational Toolkit (http://www.cactuscode.org).

[1] T. de Donder, *La Gravifique Einsteinienne* (Gauthiers-Villars, Paris, 1921).
[2] V. Fock, *The Theory of Space, Time and Gravitation* (MacMillan, New York, 1964).
[3] Y. Foures-Bruhat, Acta Math. **88**, 141 (1952).
[4] D. Garfinkle, Phys. Rev. D **65**, 044029 (2002).
[5] B. Szilágyi, B. Schmidt, and J. Winicour, Phys. Rev. D **65**, 064015 (2002).
[6] B. Szilágyi and J. Winicour, Phys. Rev. D **68**, 041501 (2003).
[7] M. C. Babiuc, B. Szilágyi, and J. Winicour, Lect. Notes Phys. **692**, 251 (2006).
[8] F. Pretorius, Classical Quantum Gravity **22**, 425 (2005).
[9] F. Pretorius, Phys. Rev. Lett. **95**, 121101 (2005).
[10] M. C. Babiuc, B. Szilágyi, and J. Winicour, gr-qc/0511154.
[11] L. Lindblom, M. A. Scheel, L. E. Kidder, R. Owen, and O. Rinne, gr-qc/0512093.
[12] M. C. Babiuc, B. Szilágyi, and J. Winicour, Phys. Rev. D **73**, 064017 (2006).
[13] B. Szilágyi, H-O. Kreiss, and J. Winicour, Phys. Rev. D **71**, 104035 (2005).
[14] H. Friedrich, Classical Quantum Gravity **13**, 1451 (1996).
[15] C. Bona, T. Ledvinka, C. Palenzuela, and M. Zácek, Phys. Rev. D **67**, 104005 (2003).
[16] H.-O. Kreiss, N. A. Peterson, and J. Yström, SIAM J. Numer. Anal. **40**, 1940 (2002).
[17] H.-O. Kreiss and O. E. Ortiz, Lect. Notes Phys. **604**, 359 (2002).
[18] A. E. Fisher and J. E. Marsden, Commun. Math. Phys. **28**, 1 (1972).
[19] H.-O. Kreiss, N. A. Petersson, and J. Yström, SIAM J. Numer. Anal. **42**, 1292 (2004).
[20] R. Arnowitt, S. Deser, and C. Misner, in *Gravitation: An Introduction to Current Research*, edited by L. Witten (Wiley, New York, 1962).
[21] M. Alcubierre and B. Schutz, J. Comput. Phys. **112**, 44 (1994).
[22] G. Calabrese, Phys. Rev. D **71**, 027501 (2005).
[23] G. Calabrese and C. Gundlach, gr-qc/0509119.
[24] M. Alcubierre and B. Brugmann, Phys. Rev. D **63**, 104006 (2001).
[25] H.-O. Kreiss and N. A. Petersson, SIAM J. Sci. Comput. **27**, 1141 (2006).
[26] H. P. Pfeiffer, L. E. Kidder, M. A. Scheel, and S. A. Teukolsky, Comput. Phys. Commun. **152**, 253 (2003).
[27] M. A. Scheel, A. L. Erickcek, L. M. Burko, L. E. Kidder, H. P. Pfeiffer, and S. A. Teukolsky, Phys. Rev. D **69**, 104006 (2004).
[28] G. Calabrese, L. Lehner, O. Reula, O. Sarbach, and M. Tiglio, Classical Quantum Gravity **21**, 5735 (2004).
[29] L. Lehner, D. Neilsen, O. Reula, and M. Tiglio, Classical Quantum Gravity **22**, 5283 (2005).
[30] H.-O. Kreiss and J. Lorenz, *Initial-boundary Value Problems and the Navier-Stokes Equations*, reprint of the 1989 edition (SIAM, Philadelphia, PA, 2004).
[31] B. Gustafsson, H.-O. Kreiss, and J. Oliger, *Time Dependent Problems and Difference Methods* (A Wiley-Interscience Publication, New York, 1995).
[32] H.-O. Kreiss and L. Wu, Applied Numerical Mathematics **12**, 213 (1993).